



Cite this: *Mater. Adv.*, 2026, 7, 144

## Sustainable photoluminescent cellulose composites for next-generation intelligent packaging

Weijing Yuan,<sup>a</sup> Hongda Guo,<sup>\*b</sup> Xue Liu<sup>\*b</sup> and Zhijun Chen<sup>b</sup>

Cellulose and its derivatives play a vital role in the preparation of food packaging materials. The properties of renewability, biodegradability, high strength, and functionalization have made them an ideal substitute for traditional petroleum-based materials and they are widely used in the development of high-performance, environmentally friendly, and functional materials. Due to their applications in freshness monitoring, anti-counterfeiting, intelligent packaging, and other areas, photoluminescent cellulose materials have undergone rapid development in recent years. However, there remains a lack of comprehensive reviews systematically addressing the fundamentals of luminescence, preparation methodologies, functionalization strategies, and implementation frameworks of cellulose-based photoluminescent materials, particularly in the context of next-generation intelligent packaging. In this review, we will comprehensively introduce the development and application of cellulose-based photoluminescent materials, especially in the field of intelligent food packaging, by combining cellulose extraction, functional modification, and advanced technologies involved. By discussing the opportunities and challenges that may be faced in the future, we propose the possible development directions. We believe that this review has important guiding significance for the further development of cellulose-based photoluminescent materials in advanced packaging systems.

Received 17th August 2025,  
Accepted 12th November 2025

DOI: 10.1039/d5ma00918a

[rsc.li/materials-advances](http://rsc.li/materials-advances)

<sup>a</sup> College of Art and Design, Heilongjiang Institute of Technology, Harbin, 150050, China

<sup>b</sup> Key Laboratory of Bio-based Material Science & Technology, Northeast Forestry University, Ministry of Education, Harbin, 150040, China.  
E-mail: liuxue1106@nefu.edu.cn, ghd1042641992@163.com



Weijing Yuan

Weijing Yuan is an associate professor at the College of Art and Design, Heilongjiang Institute of Technology. She received her PhD degree from Northeast Forestry University. Her current research interests are focused on the visual communication design.



Hongda Guo

Hongda Guo is currently pursuing his PhD degree in the group of Professor Zhijun Chen at Northeast Forestry University. His research interests are focused on the preparation and application of biomass-based photoluminescent materials. He received his master's degree in organic chemistry from Shanghai Normal University.



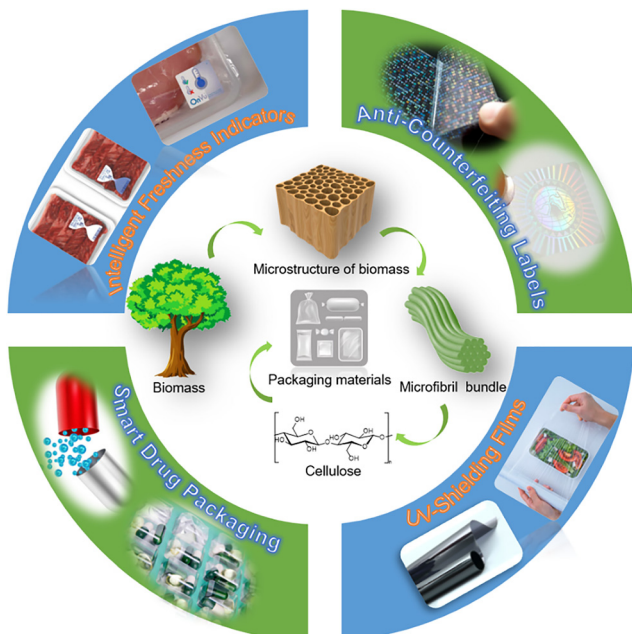


Fig. 1 An overview of the sustainable cellulose-derived photoluminescent materials and their applications in intelligent packaging.

In response to growing emphasis on low-carbon lifestyles and sustainable development, research into natural polymer-based alternatives has gained significant momentum.<sup>1</sup>

Among forest biomass components, cellulose—Earth's most abundant natural polymer—has emerged as a cornerstone for sustainable material design due to its renewability, inherent biodegradability, and tunable physicochemical properties.<sup>2–5</sup> These attributes have motivated efforts to develop lignocellulosic biopolymers for eco-friendly packaging. Recently, advances in intelligent packaging have further spurred exploration of cellulose-based systems for applications such as freshness monitoring, temperature sensing, expiration indication, and active antimicrobial control.<sup>6,7</sup>

Notably, the integration of photoluminescent functionalities into cellulose matrices has unlocked novel opportunities for intelligent packaging.<sup>8,9</sup> However, to date, most existing reviews have focused either broadly on cellulose-based materials or generally on intelligent packaging, without systematically bridging the synthesis strategies, functional mechanisms, and practical applications of photoluminescent (PL) cellulose composites. Herein, this review fills this gap by providing a systematic overview of cellulose-derived photoluminescent materials (CPLM), covering fundamental mechanisms, fabrication strategies (including nanocellulose extraction, hybrid composites, and advanced processing techniques), and their applications in intelligent packaging (*e.g.*, freshness indicators, anti-counterfeiting, UV-shielding, and drug packaging) (Fig. 1). Furthermore, we highlight emerging trends such as stimulus-responsive systems, AI-driven design, life cycle assessment, and integration with emerging technologies, offering forward-looking perspectives that have not been commonly addressed in prior literature. By systematically reviewing the CPLM for next-generation intelligent packaging, this paper aims to develop ecologically sustainable packaging solutions that concurrently address environmental concerns and intelligent functional demands.

## 2. Fundamentals of cellulose-derived photoluminescent materials (CPLM)

Cellulose nanomaterials (CNMs), including cellulose nanocrystals (CNCs) and cellulose nanofibers (CNFs), are derived from plant biomass through mechanical, chemical, or enzymatic processes.<sup>10,11</sup> Their high surface area, mechanical strength (*e.g.*, tensile strength up to 10 GPa for CNCs), and hydroxyl-rich surfaces enable facile chemical modifications, making them ideal substrates for functional composites.<sup>12–16</sup>

Photoluminescence of CPLM arises from radiative transitions of excitons returning to the ground state. Photolumines-



Xue Liu

*Xue Liu is an associate professor at the Key Laboratory of Bio-based Material Science & Technology, Northeast Forestry University. He received his PhD in materials science, specializing in wearable electronic materials and devices, from Nankai University, China, in 2024. His current research interests are focused on the fabrication and application of green flexible optical/electronic materials and devices.*



Zhiyun Chen

*Zhiyun Chen is a full professor at the Key Laboratory of Bio-based Material Science & Technology, Northeast Forestry University. He received his PhD in chemistry, with a specialization in photo-sensitive materials, from the Max Planck Institute for Polymer Research in Germany in 2017. His current research interests are focused on understanding and utilizing the PL from biomass sources and enabling the targeted conversion of biomass into optical functional materials.*



cence manifests in two distinct forms categorized by excitonic spin configurations: (1) fluorescence, mediated through singlet excitation states, and (2) phosphorescence, arising from triplet exciton transitions.<sup>17</sup> Their most distinctive distinction lies in the emission lifetimes: fluorescence occurs on the nanosecond time-scale, whereas phosphorescence persists from milliseconds to seconds due to the spin-forbidden nature of triplet-to-ground state transitions.<sup>18</sup>

## 2.1. Cellulose-derived fluorescent materials

As a typical form of photoluminescence, fluorescence arises when a substance absorbs photons and subsequently emits light at a longer wavelength. This phenomenon is typically harnessed in cellulose-derived fluorescence materials through two primary pathways: intrinsic fluorescence and extrinsic doping.

**2.1.1. Intrinsic fluorescence.** Cellulose is widely regarded as a non-fluorescent biopolymer owing to its fundamental chemical structure consisting of  $\beta$ -1,4-glucan chains. The absence of conjugated  $\pi$ -electron systems or intrinsic fluorophores in its molecular architecture provides a theoretical basis for this characteristic. However, significant fluorescence emission under specific conditions has been found, thereby challenging this conventional understanding. For example, Tang *et al.* proposed a cluster-triggered emission (CTE) mechanism to elucidate the fluorescence emission observed in cellulose systems.<sup>19</sup> Specifically, the close packing of hydroxyl groups along cellulose or its derivative polymer chains facilitates spatial conjugation between these functional groups, leading to the formation of multiple electron-delocalized clusters. These molecular clusters exhibit fluorescence emission upon photoexcitation due to stabilized excited-state transitions. Similarly, Du *et al.* synthesized and explored the photophysical properties of cellulose and its derivatives (micro-crystalline cellulose (MCC), 2-hydroxyethyl cellulose (HEC), hydroxypropyl cellulose (HPC), and cellulose acetate (CA)), finally attributing their emission to the CTE mechanism of nonconventional chromophores (e.g., hydroxyl, ether, and carbonyl groups) and

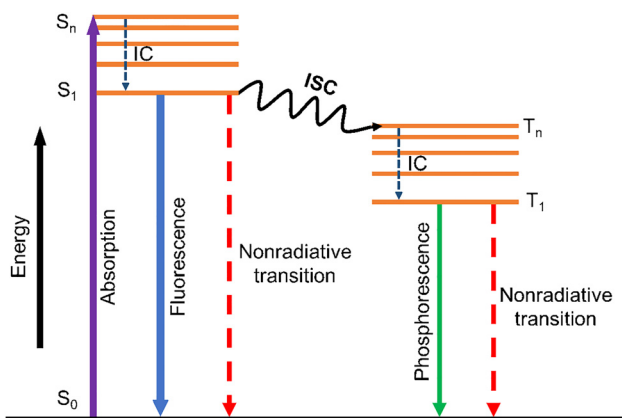


Fig. 2 Schematic diagram of the fluorescence and phosphorescence emission mechanism. Abbreviations: IC, internal conversion; ISC, inter-system conversion.

electron delocalization (Fig. 3a).<sup>20</sup> After that, utilizing cellulose acetoacetate (CAA) as the matrix for *in situ* modification, Peng *et al.* fabricated a series of fluorescent cellulose films through Hantzsch reaction-mediated incorporation of various aggregation-induced emission (AIE)-active moieties.<sup>21</sup> Finally, the fluorescent cellulose films showed a strong blue emission, which also retained processability into diverse shapes (Fig. 3b).

Furthermore, alternative physicochemical strategies have been extensively explored to harness the intrinsic fluorescence properties of cellulose-based materials. For example, Qiu *et al.* produced CAA fluorescent fibers through a lab-scale pilot wet-spinning machine, which also leveraged the CTE mechanism.<sup>22</sup> The introduction of acetoacetyl groups promoted the radiation transition while suppressing nonradiative transition processes, then the resulting fibers exhibit bright cyan-blue fluorescence emission. And the following Hantzsch or enamination reactions have been used to promote the fluorescence properties (Fig. 3c). In another study, Li *et al.* prepared a cellulose-based fluorescent hydrogel using a one-pot method *via* hydrothermal carbonization. Nanocrystalline cellulose (NCC) aqueous suspensions were subjected to hydrothermal carbonization at varying temperatures, resulting in the partial conversion of NCC into fluorescent carbon dots (CDs), and the NCC/CD hydrogel showed stable fluorescence emission at around 400–500 nm (Fig. 3d).<sup>23</sup>

Therefore, through specific mechanisms (such as cluster-triggered emission and appropriate physicochemical processing), cellulose and its derivatives can be endowed with significant intrinsic fluorescence, thereby broadening their application potential in the field of fluorescent materials.

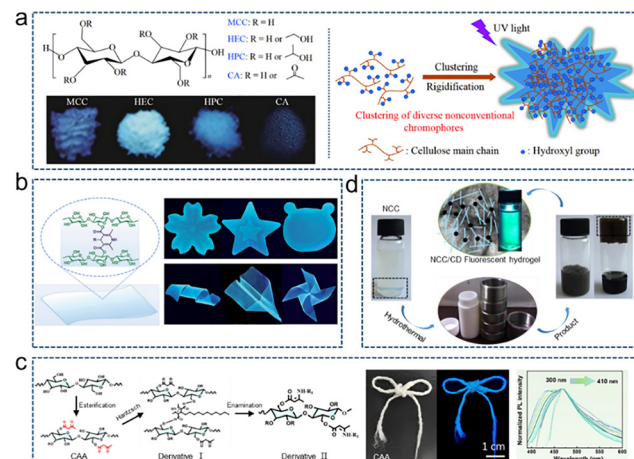


Fig. 3 Design strategy and phenomena for achieving intrinsic fluorescence of cellulose. (a) Schematic diagram of the fluorescence emission image of cellulose or its derivatives and the CTE mechanism involved. [Reproduced with permission from ref. 20. Copyright 2019 Springer Nature.] (b) Fluorescent image of cellulose films synthesized through the Hantzsch reaction. [Reproduced with permission from ref. 21. Copyright 2024 Elsevier B.V.] (c) The synthetic pathway and fluorescent image of CAA fibers. [Reproduced with permission from ref. 22. Copyright 2022 The Royal Society of Chemistry.] (d) Fluorescent image and the synthesis process of the NCC/CD hydrogel. [Reproduced with permission from ref. 23. Copyright 2017 Elsevier Ltd.]



**2.1.2. Extrinsic doping.** Cellulose could also demonstrate enhanced fluorescence performance when strategically combined with CDs through doping processes. This hybrid system capitalizes on the exceptional fluorescence properties inherent to carbon-based nanomaterials while maintaining the sustainable advantages of cellulosic substrates. For instance, Wu *et al.* demonstrate an effective strategy of constructing high-performance composite luminescent materials by doping cellulose with carbon dots. They prepared yellow-emitting carbon dots ( $\gamma$ -CDs) *via* a one-step hydrothermal process using *o*-phenylenediamine, which exhibited high water dispersivity and prominent fluorescence properties.<sup>24</sup> After doping in carboxy methyl cellulose/polyvinyl alcohol (CMC/PVA) or chitosan, the  $\gamma$ -CDs/polymer composite sensor for  $\text{Cu}^{2+}$  ions was fabricated. Upon increasing  $\text{Cu}^{2+}$  ion concentration, the composite films demonstrated enhanced blue fluorescence emission centered at approximately 450 nm (Fig. 4a). Similarly, Lv *et al.*

obtained a kind of green and simple fluorescence biosensor based on bacterial cellulose (BC).<sup>25</sup> Specifically, they synthesized N-CDs using citric acid (CA) and ethanediamine (EDA) *via* hydrothermal treatment first, and then a composite membrane was prepared after incorporating N-CDs into the BC membrane *via* the sustainable one-step method of biosynthesis. The final product presented a good sensitive response towards  $\text{Fe}^{3+}$ , which will cause quenching of fluorescence at about 450 nm (Fig. 4b). Song *et al.* constructed a fluorescent carbon quantum dot (CQD) composite aerogel *via* a one-pot method using ethylenediamine as a nitrogen source to dope nanofibrillated cellulose derived from poplar wood powder exogenously. This material not only efficiently adsorbs  $\text{Cr}^{3+}$  in water but also enables real-time visual monitoring of the adsorption process through the fluorescence quenching effect of CQDs, with the entire preparation process being environmentally friendly (Fig. 4c).<sup>26</sup> Besides, other kinds of quantum dots (QDs) were also used to achieve the fluorescence emission of cellulose. Xie *et al.* synthesized a composite film by blending cellulose nanocrystals/zinc sulphide (CNCs/ZnS) composites with PVA. Initially, CNCs were functionalized *in situ* with ZnS quantum dots, which were subsequently incorporated into a PVA matrix to fabricate nanocomposite films exhibiting dual functionality of fluorescence. And the visible emission peak in the nanocomposites was 473 nm with an excitation wavelength of 350 nm (Fig. 4d).<sup>27</sup>

Beyond carbon dots and quantum dots, owing to the unique electronic configurations and energy level characteristics, lanthanide (Ln) ions have been successfully incorporated into cellulose-based photoluminescent materials. Altam *et al.* fabricated CMC, quaternized cellulose (QC), and Ln ions ( $\text{Ce}^{3+}$ ,  $\text{Eu}^{3+}$ , and  $\text{Tb}^{3+}$ ) ternary composite thin film by hierarchical assembly. Firstly, the negatively charged polymer-metal complex nanoparticles were prepared by mixing the CMC solution and the Ln ion solution. Then, the thin films were fabricated by layer-by-layer (LBL) assembly between negatively charged CMC@Ln nanoparticles and positively charged QC chain, and the corresponding films showed blue, green, and red fluorescence color under UV irradiation (Fig. 4e).<sup>28</sup> Feng *et al.* synthesized fluorescent nanocellulose (PCNF) using pyrenetetracarboxylic acid (PTCA), and subsequently, cellulose fluorescent hydrogels were prepared *via* salting-out. More importantly, the hydrogel fluorescence showed tunable emission by altering the ligand metal type ( $\text{Eu}^{3+}$  and  $\text{Tb}^{3+}$ ), resulting in red, greenish-yellow, and yellow fluorescence under 365 nm UV illumination when Eu-PTCA, Tb-PTCA, and Eu-PTCA/Tb-PTCA ligands were present, respectively (Fig. 4f).<sup>29</sup>

The above research study has proved that by doping functional nanomaterials such as carbon dots, quantum dots, or lanthanide ions into cellulose systems, researchers have successfully prepared a series of composite materials with excellent fluorescence properties, expanding their potential for application in ion sensing and intelligent monitoring.

## 2.2. Cellulose-derived phosphorescent materials

Compared to fluorescence, phosphorescence exhibits extended lifetimes and large Stokes shifts, enabling sustained emission

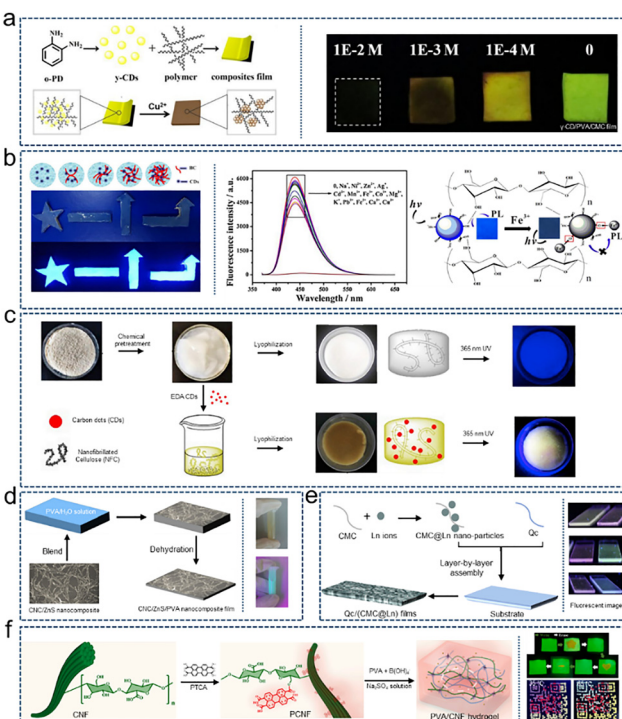


**Fig. 4** Design strategy and phenomena for achieving extrinsic fluorescence of cellulose. (a) Preparation process of  $\gamma$ -CD/PVA/CMC film and fluorescent image of the film interacting with  $\text{Cu}^{2+}$ . [Reproduced with permission from ref. 24. Copyright 2013 The Royal Society of Chemistry.] (b) Fluorescence imaging of bacterial cellulose loaded carbon dot composite materials and the mechanism of specific recognition of  $\text{Fe}^{3+}$ . [Reproduced with permission from ref. 25. Copyright 2017 Elsevier Ltd.] (c) Fabricating process and fluorescent properties of nanofibrillated cellulose and NFC loaded CD composite. [Reproduced with permission from ref. 26. Copyright 2020 Elsevier B.V.] (d) Preparation process of CNC/ZnS/PVA nanocomposite film and the fluorescence spectra. [Reproduced with permission from ref. 27. Copyright 2019 Springer Nature B.V.] (e) Preparation process of Qc/(CMC@Ln) films and fluorescence imaging. [Reproduced with permission from ref. 28. Copyright 2017 Elsevier Ltd.] (f) Production process of the PVA/CNF hydrogel and the fluorescent image of anti-counterfeiting. [Reproduced with permission from ref. 29. Copyright 2024 Elsevier B.V.]



after excitation cessation (Fig. 2).<sup>30</sup> The unique characteristics mentioned above, particularly the persistent emission and minimal signal interference from large Stokes shifts, have propelled photoluminescence materials into diverse applications, including intelligence monitoring, data encryption, anti-counterfeiting labeling, chemical sensing, and persistent luminescence displays. These properties allow for time-gated detection to eliminate background noise, enable delayed readouts for information security, and facilitate sustained emission without the need for constant excitation.

**2.2.1. Cellulose as an intrinsic phosphor.** The abundance of functional groups (*e.g.*, hydroxyl, amino, and carboxyl) within cellulose's structure creates a favorable, rigid environment conducive to its intrinsic RTP. Furthermore, the synergistic effect of introducing heteroatoms and/or unsaturated subunits can successfully activate intrinsic RTP emission in cellulose. The construction of cellulose-based RTP materials primarily utilizes two strategies: leveraging inherent crystallization or employing chemical modification.<sup>31</sup> For instance, Zhou *et al.* investigated the RTP behavior of MCC by modulating its crystallinity and crystal morphology. Their results revealed that MCC exhibits non-traditional RTP emission governed by a clusteroluminescence mechanism. Notably, the quantum efficiency and lifetime of the RTP correlated directly with changes in crystallinity.<sup>32</sup> Alternatively, chemical modification can be employed to introduce electron-rich functional groups (such as carbonyl ( $-\text{C}=\text{O}$ ), carboxyl ( $-\text{COOH}$ ), and imine ( $-\text{C}=\text{N}-$ )) into the cellulose polysaccharide chains. This approach effectively enhances the ISC process, thereby promoting RTP emission.<sup>33</sup> As an example, Zhang *et al.* grafted imidazolium cations ( $\text{Im}^+$ ) paired with chloride anions ( $\text{Cl}^-$ ), as well as imidazolium cations functionalized with phenyl carboxylate ester substituents, onto the cellulose backbone. This modification simultaneously enhanced ISC and suppressed non-radiative transitions, ultimately yielding various cellulose derivatives exhibiting significant RTP performance.<sup>34-36</sup>

**2.2.2. Cellulose as a rigid matrix for guest phosphors.** RTP in cellulose-derived rigid matrices can be engineered through various interactions, including hydrogen bonding, halogen bonding, ionic bonding, and covalent bonding.<sup>31</sup> For example, Gao *et al.* employed a heterogeneous boron–oxygen covalent strategy to incorporate aryl-boronic acid chromophores directly onto the cellulose framework, producing multi-color, long-lifetime phosphorescent cellulose materials.<sup>37</sup> Similarly, Peng *et al.* utilized the Hantzsch reaction to *in situ* graft 1,4-dihydropyridine derivatives (DHPs) onto acetylated cellulose. By introducing diverse aromatic substituents to modulate the conjugation degree, they achieved tunable RTP emission in cellulose derivatives.<sup>38</sup>

**2.2.3. Cellulose as a precursor for phosphorescent carbon dots (CDs).** In addition to serving as a chromophore or a rigid matrix to construct RTP composite materials, natural polysaccharides, such as cellulose, can also serve as precursors for CDs. Under appropriate conditions, these polysaccharides undergo ring-opening reactions. Subsequent dehydration and oxidation yield reactive aldehydes. Within the resulting CD

structure, the  $n \rightarrow \pi^*$  transition of surface functional groups promotes ISC, thereby populating triplet excitons and generating significant RTP emission.<sup>39</sup> For example, researchers have demonstrated that direct hydrothermal cross-linking of CMC and EDA yields CMC-based RTP CDs (denoted as CMC CDs). This approach significantly expands the scope of applications for cellulose-derived RTP materials.<sup>40</sup>

In summary, the fabrication of cellulose-based fluorescent materials primarily relies on either intrinsic fluorescence or the incorporation of external fluorophores. In the case of cellulose-based phosphorescent materials, phosphorescence can be achieved not only by controlling crystallization or introducing electron-rich groups to activate intrinsic emission, but also by utilizing cellulose as a rigid host matrix or as a carbon dot precursor. The preparation of cellulose-based phosphorescent materials is more complex and diverse. Cellulose-based fluorescent materials offer advantages such as rapid response, diverse synthesis routes, ease of functionalization, and compatibility with various nanomaterials. However, they typically suffer from short emission lifetimes, susceptibility to background fluorescence, photobleaching, and limited stability. In contrast, cellulose-based phosphorescent materials exhibit longer emission lifetimes and larger Stokes shifts, which help to effectively minimize interference from background light. It should be noted, however, that these materials often require a rigid microenvironment to suppress non-radiative transitions and are also vulnerable to quenching by external factors such as moisture and oxygen. Based on the versatile optical properties and structural characteristics of cellulose nanomaterials, the fundamental understanding of CPLM lays the crucial groundwork for their advanced fabrication methods and intelligent applications, which will be elaborated in the following sections.

### 3. Fabrication strategies for CPLM

The standard fabrication process for CPLM typically comprises three parts: the preparation of nanocellulose with initial PL, the synthesis of cellulose-derived hybrid composites, and advanced processing techniques, which will accelerate their scale production. This section examines the underlying mechanisms and presents representative implementation of these three strategic phases.

#### 3.1. Nanocellulose extraction and functionalization

**3.1.1. Acid hydrolysis.** Acid hydrolysis of native cellulose with a mineral acid, for example, concentrated sulfuric acid, is a well-known and effective process for degrading amorphous cellulose to produce well-defined nanocellulose.<sup>41-43</sup> But it presents significant environmental and toxicological hazards while simultaneously inducing corrosive degradation of processing equipment. Consequently, there is a growing trend toward utilizing greener alternatives such as organic acids, which not only mitigate environmental impact but also introduce functional groups that enhance the applicability of nanocellulose in advanced materials. Based on this, Ji *et al.* used an innocuous



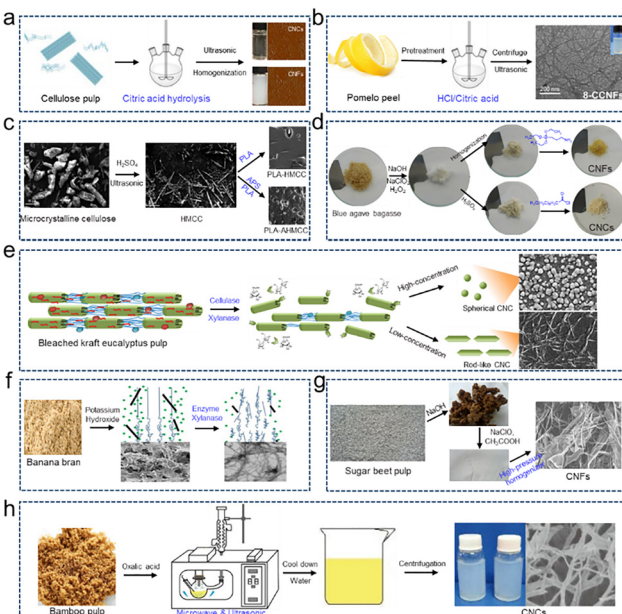


**Fig. 5** Extraction strategy of nanocellulose. (a) and (b) Schematic description of the acid hydrolysis of cellulose. [Reproduced with permission from ref. 44. Copyright 2013 The Royal Society of Chemistry and reproduced with permission from ref. 45. Copyright 2021 Springer Nature B.V.] (c) and (d) Schematic diagram of the modifications of cellulose to enhance the compatibility with PL agents. [Reproduced with permission from ref. 46. Copyright 2011 Wiley and reproduced with permission from ref. 47. Copyright 2015 Elsevier B.V.] (e) and (f) Schematic description of the enzymatic treatments of cellulose. [Reproduced with permission from ref. 48. Copyright 2019 Wiley and reproduced with permission from the ref. 49. Copyright 2014 Elsevier Ltd.] (g) and (h) Schematic diagram of the involved mechanical treatments of cellulose. [Reproduced with permission from ref. 50. Copyright 2013 Elsevier Ltd.]

weak acid (citric acid) to prepare CNCs and CNFs from bleached bagasse pulp, accompanied by simultaneous modifications of the carboxylic group on their molecular interface *via* esterification.<sup>44</sup> This strategy exemplifies a green one-step pathway that integrates hydrolysis and carboxylation, addressing both sustainability and functionality. Finally, CNCs with a diameter of 20–30 nm and length of 250–450 nm, and CNFs with a diameter of 30–60 nm and length of 500–1000 nm were achieved, and over 90% of the citric acid was recovered by rotary evaporator (Fig. 5a). The high recovery rate underscores the economic and environmental viability of citric acid as a hydrolyzing agent and thus making it particularly attractive for scalable production. Li *et al.* developed a one-step acid hydrolysis protocol utilizing a hydrochloric acid/citric acid (HCl/CA) binary system to directly extract carboxylated cellulose nanofibers (CCNFs) *via* esterification reaction from pomelo peel waste.<sup>45</sup> This approach not only valorizes agricultural residues but also introduces carboxyl groups that significantly improve the dispersibility and stability of the resulting nanofibers in aqueous systems. The prepared CCNFs entangled with each other showed diameters of 5–15 nm and lengths of 0.8–1.2  $\mu\text{m}$ , depending on the CA content (Fig. 5b). It is noteworthy that the aspect ratio and surface charge of CCNFs can be tailored by

adjusting the HCl/CA ratio, which directly influences their performance in applications such as Pickering emulsions. Except for esterification, CNCs produced with high crystallinity can be further modified *via* surface silanization to enhance compatibility with PL agents. Frone *et al.* synthesized polymer composites from polylactic acid (PLA) and microcrystalline cellulose (HMCC). They performed a surface treatment of cellulose fibers based on 3-aminopropyltriethoxysilane (APS), so that the compatibility with the PLA matrix was enhanced. As a result, the composites showed a higher enhancement of storage modulus, which allows better matrix–filler stress transfer (Fig. 5c).<sup>46</sup> This enhancement is attributed to the improved interfacial adhesion and reduced agglomeration of fibers, which facilitate more efficient stress transfer from the polymer matrix to the reinforcing phase. Robles *et al.* modified the surface hydrophilicity of CNFs and CNCs by using APS and dodecanoyl chloride, respectively, and obtained different composite materials with the PLA matrix.<sup>47</sup> These modifications enhanced the mechanical properties and hydrophobicity of the material, as well as the dispersion of fillers within the matrix (Fig. 5d). Comparative analysis of these two modification strategies reveals that while silanization improves interfacial compatibility through covalent bonding, esterification with long-chain fatty acids imparts greater hydrophobicity and ductility, thereby expanding the potential for application of nanocellulose in biodegradable composites.

Collectively, these studies highlight a paradigm shift from conventional mineral acid hydrolysis to multifunctional and environmentally benign extraction methods. The integration of hydrolysis with *in situ* functionalization not only streamlines the production process but also tailors the surface chemistry of nanocellulose for specific applications, particularly in sustainable packaging and biocomposites.

**3.1.2. Enzymatic/mechanical treatments.** Enzymatic hydrolysis has emerged as a critically important approach for nanocellulose extraction due to its exceptional environmental compatibility, remarkable selectivity, and precise control over product characteristics. Different from conventional chemical methods employing harsh acids, enzymatic processes operate under mild conditions, minimizing degradation of cellulose and preserving its native structure. Tong *et al.* prepared CNCs using different morphologies (spherical and rod-like) *via* the compound enzymolysis (cellulase and xylanase) method from eucalyptus cellulose fiber.<sup>48</sup> Their systematic investigation revealed that by adjusting the enzyme ratio, total enzyme concentration, and hydrolysis time, the morphology of CNCs could be precisely tailored. Specifically, spherical CNCs were favored under high cellulose concentration and extended hydrolysis, whereas rod-like CNCs dominated when xylanase was predominant. These results illustrate the synergistic role of cellulase in hydrolyzing amorphous regions and xylanase in enhancing cellulose accessibility, providing a green pathway for morphology-controlled CNC synthesis (Fig. 5e). Tibolla *et al.* produced CNFs from banana peel bran *via* chemical treatment (CT–alkaline treatment, bleaching, and acid hydrolysis) and enzymatic treatment (ET–alkaline treatment and hydrolysis



with xylanase).<sup>49</sup> Comparative analysis demonstrated that despite yielding less pure nanofibers, ET achieved a higher production yield than CT, highlighting the efficiency and sustainability of enzymatic approaches. In addition, as indicated by zeta potential measurements, ET-produced CNFs exhibited higher aspect ratios and better colloidal stability, which are critical for reinforcement in nanocomposites. CNFs derived from CT and ET exhibited distinct morphological characteristics, with average diameters of 10.9 nm and 7.6 nm, and lengths of 454.9 nm and 2889.7 nm, respectively, which showed potential for composite applications (Fig. 5f). Meanwhile, mechanical methods, including high-pressure homogenization (HPH), grinding, and high-intensity ultrasonic treatment, can also be exploited to extract CNFs from plant cell walls. These techniques primarily exert physical forces to disintegrate fiber bundles into nanoscale fibrils, often in combination with chemical or enzymatic pretreatments to reduce energy consumption. Li *et al.* produced cellulose nanofibers (diameter = 10–70 nm) *via* chemical treatments (alkali treatment and bleaching) and high-pressure homogenization from de-pectinated sugar beet pulp (DSBP).<sup>50</sup> The sequential application of chemical purification and HPH not only removed non-cellulosic components effectively but also significantly enhanced the crystallinity and thermal stability of the resulting CNFs. This underscores the synergistic effect of chemical and mechanical treatments in producing high-performance nanocellulose suitable for demanding applications. The obtained DSBP-derived CNFs exhibited superior thermal degradation temperatures, demonstrating their potential as high-performance reinforcing agents in bio-composites for elevated-temperature applications (Fig. 5g). Lu *et al.* fabricated CNCs *via* a one-step procedure using melt oxalic acid hydrolysis and treating with microwaves and ultrasonic waves simultaneously.<sup>51</sup> This innovative approach, integrating hydrolysis and esterification in a solvent-free system, represents a significant advancement in green synthesis, in which one could achieve nanocrystallization and functionalization simultaneously. The method not only attained a high yield of 85.5% but also produced carboxylated CNCs with excellent thermal stability and dispersion stability, addressing the common limitations of traditional acid hydrolysis (Fig. 5h). Collectively, these studies illustrate the evolving trend toward integrating multiple techniques—enzymatic, chemical, and mechanical—to optimize the yield, properties, and functionality of nanocellulose. The ability to tailor morphology, enhance thermal stability, and introduce surface functionalization through these hybrid methods significantly expands the application potential of nanocellulose in advanced materials.

### 3.2. Hybrid composite synthesis

Beyond initial PL, adopting composite material strategies enables significant enhancement of photoluminescence properties of cellulose while improving its processability. This section delineates two cellulose-based hybrid systems established through *in situ* synthesis and post-modification approaches.

**3.2.1. In situ synthesis.** Cellulose-based photoluminescent materials represent a class of functional composites formed

through *in situ* synthesis of luminescent nanoparticles (*e.g.*, ZnS and CdSe) within the cellulose matrix. These systems are characterized by utilizing cellulose's three-dimensional network architecture as either a structural template or supporting substrate, enabling both uniform dispersion of the luminescent species and enhanced material stability. Luna-Martínez *et al.* prepared ZnS–sodium carboxymethyl cellulose nanocomposite films by casting after the *in situ* precipitation of ZnS in sodium carboxymethyl cellulose (NaCMC) aqueous solution.<sup>52</sup> NaCMC served as a stabilizer to prevent nanoparticle aggregation, yielding ZnS quantum dots of about 3 nm. Due to sulfur vacancies of ZnS, the nanocomposite films exhibit a visible emission band centered at 445 nm under a 320 nm UV lamp, which may have a potential for application in anti-counterfeiting (Fig. 6a). Furthermore, in another research study *in situ* synthesis, Yang *et al.* fabricated flexible luminescent membranes based on BC by the *in situ* synthesis of the CdSe nanoparticles on the BC nano-fibers.<sup>53</sup> Cellulose matrix provided a framework for CdSe to disperse homogeneously. CdSe nanoparticles endow this composite material with good stability and PL properties simultaneously, which showed a significant emission peak at 529 nm. And the films are promising for applications in the fields of sensors and flexible luminescent membranes (Fig. 6b).

**3.2.2. Post-modification.** Post-modification of cellulose represents a critical post-functionalization strategy that enhances compatibility between cellulose matrices and luminescent components, improves material stability, and confers multifunctional

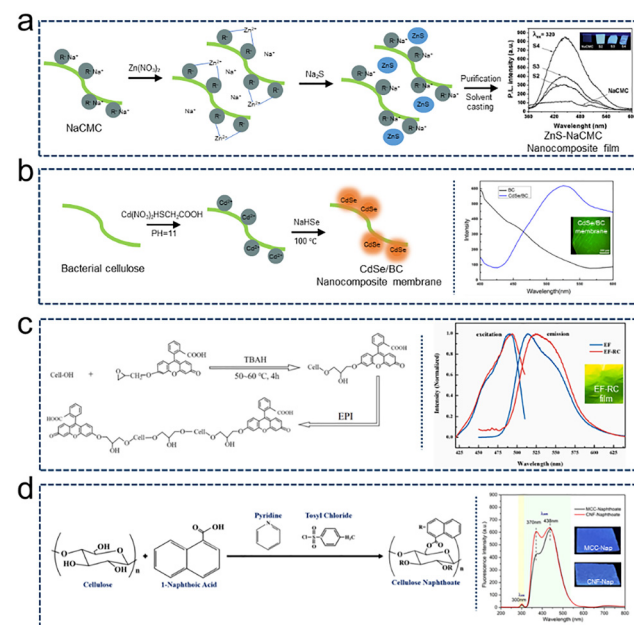


Fig. 6 Synthetic strategy of PL cellulose hybrid composites. (a) and (b) *In situ* synthesis of PL cellulose-derived composites using cellulose and luminescent nanoparticles. [Reproduced with permission from ref. 52. Copyright 2010 Elsevier Ltd and reproduced with permission from ref. 53. Copyright 2011 Elsevier Ltd.] (c) and (d) Post-modification of cellulose through various reactions. [Reproduced with permission from ref. 54. Copyright 2020 Elsevier Ltd.]



characteristics. Shi *et al.* prepared several cellulose films using a special tetra-butylammonium hydroxide TBAH/H<sub>2</sub>O/DMSO ternary solvent system.<sup>54</sup> This system contributed the rapid dissolution of high-DP cellulose and allowed subsequent covalent grafting of modified fluorescein, yielding films with excellent fluorescence stability, pH response, and for the first time, polarized emission after stretching (Fig. 6c). Besides, Lease *et al.* produced fluorophore-labeled cellulose after modifying MCC and CNFs.<sup>55</sup> Esterification with 1-naphthoic acid (1-NA) resulted in cellulose naphthoates with a degree of substitution of up to 1.55, inducing a strong indigo fluorescence under UV and reducing crystallinity while suggesting potential melt-processability (Fig. 6d).

### 3.3. Advanced processing techniques

Advanced processing technologies have enabled the scale-up of photoluminescent cellulose composites beyond laboratory confines, with their technical evolution now characterized by multi-scale precision control (e.g., additive manufacturing), green manufacturing protocols (e.g., biomass raw materials), and intelligent system integration (e.g., electrospinning). This section specifically examines the implementation of 3D printing and electrospinning techniques in developing photoluminescent cellulose-based materials.

**3.3.1. Electrospinning.** Electrospinning is an advanced manufacturing technique that utilizes high-voltage electrostatic forces to fabricate continuous micro/nanoscale fibers from polymer solutions or melts. For example, Ravichandran *et al.* produced novel green organic-inorganic hybrid nanofibers (NiO@CA) using the electrospinning technique.<sup>56</sup> These nanofibers are composed of NiO nanoparticles that exhibit UV absorption at 276 nm, which are integrated into cellulose acetate nanofibers, and the nanofibers can function as anti-microbial packaging for food preservation, owing to the intrinsic antibacterial activity of the embedded NiO nanoparticles (Fig. 7a). Furthermore, Yang *et al.* presented a novel sensor based on phospholipid membrane-encapsulated perovskite quantum dots, after integrating them onto a glass cellulose membrane using electrospinning.<sup>57</sup> The developed sensor undergoes a substitution reaction with ammonia and shows a significant decrease in the fluorescence intensity after undergoing a substitution reaction with ammonia, which can be used for non-invasive detection of *Helicobacter pylori* (Fig. 7b).

**3.3.2. 3D printing.** 3D printing, more formally termed additive manufacturing, is a digital fabrication technology that constructs three-dimensional objects through sequential, layer-by-layer material deposition. Tang *et al.* prepared several 3D printing inks by using polyvinyl alcohol (PVA) and polysaccharides (e.g., carboxymethyl cellulose).<sup>58</sup> Because bromothymol blue (BTB) and methyl red (MR) are pH-sensitive indicators, the 3D printed labels produced from these inks successfully monitored the changes in CO<sub>2</sub> concentration (which affects the package's internal pH) within tomato packaging during storage (Fig. 7c). Meanwhile, Zhan *et al.* proposed a novel gel that contained hydroxymethyl cellulose and anthocyanins, which can be used for 3D/4D printing.<sup>59</sup> Because anthocyanins have

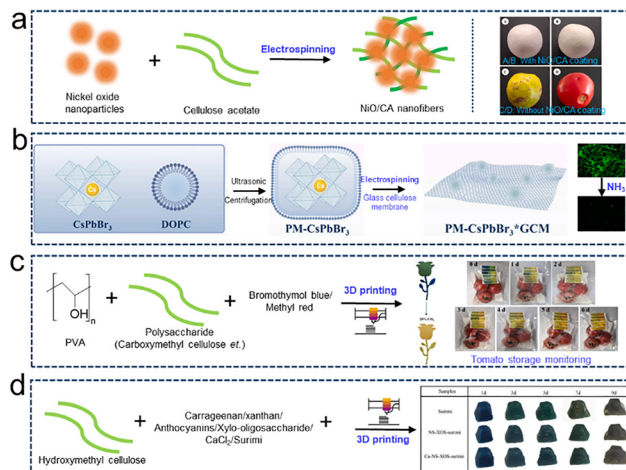


Fig. 7 Advanced processing techniques for fabricating cellulose-derived composite materials. (a) and (b) Electrospinning for cellulose-based antibacterial and gas monitoring materials. [Reproduced with permission from ref. 56. Copyright 2025 Elsevier Ltd and reproduced with permission from ref. 57. Copyright 2025 Elsevier B.V.] (c) and (d) 3D printing technique for preparing cellulose-based materials for food fresh monitoring. [Reproduced with permission from ref. 58. Copyright 2024 Elsevier Ltd and reproduced with permission from ref. 59. Copyright 2023 Elsevier Ltd.]

different color characteristics at different pH levels, the freshness of surimi can be monitored through color change (Fig. 7d).

Overall, these diverse fabrication strategies—spanning nanocellulose extraction, hybrid composite synthesis, and advanced processing—collectively provide scalable, tunable platforms for developing high-performance CPLM, and also pave the way for their practical implementation in next-generation intelligent packaging systems.

## 4. Applications of CPLM in intelligent packaging

The unique optical properties of CPLM have enabled their deployment in a variety of intelligent packaging systems, which leverage their responsiveness to environmental stimuli for real-time monitoring and enhanced functionality. Their tunable optical characteristics, inherent biodegradability, and exceptional processability make them promising as sustainable alternatives to conventional petroleum-based materials. Herein, in this section, we discuss the current advancements in cellulose-based photoluminescent composites, with a particular emphasis on their demonstrated applications in packaging.

### 4.1. Intelligent freshness indicators

PL composites responsive to pH or gas changes (e.g., NH<sub>3</sub> from spoiled meat) enable real-time food quality monitoring. The underlying mechanism relies on the interaction between the photoluminescent probes and the target analytes (e.g., gases and pH changes), which alters the electronic structure or energy transfer pathways of the probes, and finally leads to measurable changes in fluorescence/phosphorescence intensity,



lifetime, or emission wavelength. For example, Xu *et al.* fabricated a cellulose-based fluorescent functional material with dual-responsive properties. Specifically, they grafted poly (lactic acid) and 7-hydroxy-4-trifluoromethyl coumarin (HFC) onto the cellulose backbone in a CO<sub>2</sub>-switchable solvent.<sup>60</sup> Owing to the coordination between Fe<sup>3+</sup> ions and the carbonate linkage groups, non-radiative electron or energy transfer effectively suppressed the fluorescence emission and as a result, the obtained material, C-g-PLLA/HFC, showed fluorescence quenching response to Fe<sup>3+</sup>. Subsequently, the hydroxyl groups on HFC were acetylated to obtain the final material C-g-PLLA/HFC-Ac. When this material encounters organic amines, the acetyl groups are removed through an aminolysis reaction, restoring the strong fluorescence of the fluorophore HFC and thus exhibiting a “turn-on” fluorescence enhancement response. The sensing mechanism lies in the irreversible generation of luminescent HFC through amidolysis, rather than the enhancement of intramolecular charge transfer due to deprotonation or hydrogen bonding. This property enables it to be used as an intelligent indicator for monitoring the freshness of aquatic products (Fig. 8a). In a separate approach focusing on phosphorescence, Peng *et al.* synthesized cellulose-based RTP derivatives incorporating *in situ* formed DHPs. By utilizing water molecules to disrupt the rigid hydrogen-bonded network of cellulose, they achieved reversible quenching and recovery of phosphorescence. Specifically, with the increase of humidity, water molecules penetrate the cellulose matrix, breaking the rigid hydrogen bonds that suppress molecular vibration and non-radiative decay. This increased molecular motion promotes the non-radiative deactivation of triplet excitons, leading to phosphorescence quenching. Conversely, when the environment dries, the hydrogen-bonded

network reforms, restoring the rigid matrix and enabling persistent RTP emission.<sup>38</sup>

#### 4.2. Anti-counterfeiting labels

UV-activated PL patterns on cellulose-based tags provide tamper-evident solutions for luxury goods and pharmaceuticals. For instance, Zhang *et al.* demonstrated an eco-friendly co-assembly strategy for fabricating large-area, quadruple-level chiral luminescent materials by embedding poly(ethylene glycol)-stabilized lanthanide complexes within chiral nematic CNC films.<sup>61</sup> The PEG matrix facilitates uniform dispersion of Eu(DPA)<sub>3</sub> complexes, while the left-handed chiral nematic structure of CNC induces right-handed circularly polarized luminescence with an asymmetric factor exceeding -0.36. The composite exhibits a long fluorescence lifetime of 510 μs and a high absolute quantum yield of 66.7%, indicative of excellent photostability and energy conversion efficiency. Moreover, the material displays multiple optical states—structural color, fluorescence, CPL, and polarization-angle-dependent color switching—enabling multimodal anti-counterfeiting. Notably, the film also shows reversible humidity-responsive behavior, further enhancing its potential for dynamic security labeling. The brightest fluorescent film thus serves as a high-level anti-counterfeiting label on model banknotes, combining sustainability with sophisticated optical encryption (Fig. 8b). Gao *et al.* developed a facile heterogeneous B–O covalent bonding strategy to anchor arylboronic acid chromophores onto cellulose chains in pure water, resulting in multicolor RTP cellulose. The B–O covalent bonds, combined with hydrogen bonds, created a rigid matrix that restricted molecular motion of the chromophores, thereby promoting intersystem crossing (ISC) and suppressing non-radiative transitions, which led to long-lived RTP emission lifetimes of 1.42 s. By varying the π-conjugation degree of the arylboronic acids, the afterglow color could be tuned from blue to green and then to red. Building on this, they incorporated the chromophore as an additive into the pulp during the paper-making process, using a Fast Kaiser process-forming machine to achieve large-scale production of phosphorescent paper. The RTP paper exhibited water-responsive properties enabling reversible on–off switching for applications in rewritable encryption and anti-counterfeiting.<sup>37</sup>

#### 4.3. UV-shielding films

Ultraviolet radiation accelerates food oxidation and nutrient degradation, necessitating the application of cellulose-based UV-shielding films in food packaging to extend shelf life. Cellulose-based photoluminescent composites, particularly those incorporating inorganic nanoparticles such as zinc oxide (ZnO), exhibit excellent UV-blocking capabilities due to their ability to absorb and scatter UV radiation. The mechanism involves the wide bandgap of ZnO (~3.3 eV), which enables strong absorption in the UV region (200–400 nm). Upon UV excitation, electrons are promoted from the valence to the conduction band, and the absorbed energy is subsequently dissipated as heat or re-emitted as lower-energy visible or infrared radiation, thereby reducing UV penetration. Boopasiri

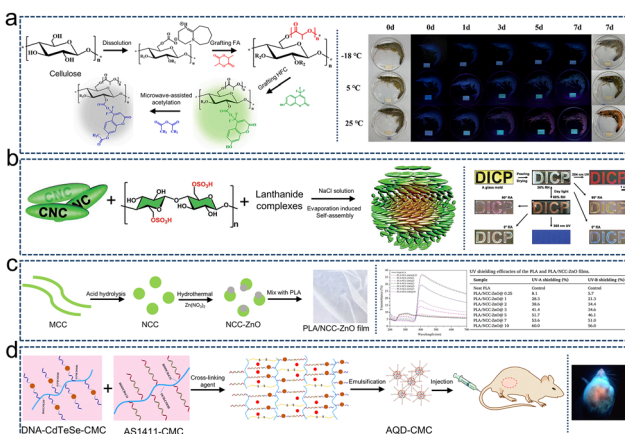


Fig. 8 Advanced applications of cellulose-derived materials in packaging. (a) Seafood freshness monitoring images and the fabrication process of cellulose-based freshness monitoring materials. [Reproduced with permission from ref. 60. Copyright 2023 Elsevier B.V.] (b) Preparation of cellulose-based anti-counterfeiting materials and their application in this aspect. [Reproduced with permission from ref. 61. Copyright 2022 Wiley.] (c) Production of cellulose-based UV-shielding materials and their application in UV-shielding. [Reproduced with permission from ref. 62. Copyright 2023 Elsevier Ltd.] (d) Application of cellulose-derived materials in drug packaging [Reproduced with permission from ref. 63. Copyright 2022. The Royal Society of Chemistry.]



Table 1 Performance comparison of representative CPLM in intelligent packaging applications

Material composition	Application	PL type	Emission wavelength	Target analyte/function	PL stability	Ref.
CAA-DHPs derivative films	4.1 Intelligent freshness indicators	RTP	Tunable (blue to red)	Water	Irreversible RTP modulated by moisture	38
C-g-PLLA/HFC-Ac	4.1 Intelligent freshness indicators	Fluorescence	500 nm	Organic amines	Irreversible response	60
Cellulose/arylboronic acid	4.2 Anti-counterfeiting labels	RTP	Tunable (blue to red)	Anti-counterfeiting, rewritable encryption	Irreversible RTP modulated by moisture	37
CNC/Eu(DPA) <sub>3</sub> chiral nematic film	4.2 Anti-counterfeiting labels	Fluorescence & CPL	~614 nm	Anti-counterfeiting	Excellent photostability; complex fabrication	61
PLA/NCC-ZnO composite film	4.3 UV-shielding films	N/A	N/A	UV-blocking	N/A	62
CMC/DNA-CdTeSe QDs nanohydrogel	4.4 Smart drug packaging	Fluorescence	~703 nm	Cancer cell targeting, drug delivery tracking	Excellent stability	63

*et al.* built composite films based on biodegradable poly (lactic acid) (PLA) incorporated with NCC and nanocrystalline cellulose coated with zinc oxide (NCC-ZnO).<sup>62</sup> NCC was first extracted from microcrystalline cellulose *via* acid hydrolysis, and then served as a supporting substrate for the *in situ* growth of ZnO nanoparticles through a hydrothermal process. This hierarchical structure not only improved the dispersion of ZnO within the polymer matrix but also enhanced the interfacial compatibility, leading to synergistic reinforcement and functional properties. After doping into PLA, the NCC-ZnO composite film showed a high UV-shielding efficacy with a significant reduction in transmittance in both UV-A (320 nm) and UV-B (280 nm) regions, reaching up to 60% and 56% shielding, respectively, at a 10 phr loading, while maintaining high transparency in the visible light range. This combination of high UV protection and optical clarity makes such composites ideal for protecting light-sensitive products (Fig. 8c).

#### 4.4. Smart drug packaging

PL hydrogels with controlled drug release (*e.g.*, cellulose aerogels) enable traceable delivery systems in medical packaging. To address the challenges of active tumor targeting, fluorescence tracking, and controlled drug release, Zheng *et al.* developed multifunctional CMC-based fluorescent nanohydrogels for nanocarriers based on near-infrared ssDNA1-templated CdTeSe QDs (DNA1-CdTeSe QDs), building block.<sup>63</sup> The nanocarrier was constructed through DNA-directed self-assembly: DNA1-CdTeSe QDs and an AS1411 aptamer (DNA2) were grafted onto CMC chains, which were then crosslinked *via* complementary DNA hybridization and disulfide bonds to form the hydrogel network. The nanohydrogel carriers showed a diameter of about 150 nm and a drug loading rate of 84.05%. These carriers exhibited active targeting to cancer cells *via* the AS1411 aptamer. Based on this, the controlled drug release was triggered by the tumor microenvironment, specifically through the cleavage of disulfide bonds by glutathione (GSH) and strand displacement induced by miRNA. Moreover, the embedded DNA1-CdTeSe QDs, with an emission center at 650 nm, served as a stable near-infrared fluorescent probe, allowing the entire drug delivery process to be monitored in real time *via* fluorescence imaging (Fig. 8d).

Collectively, these applications demonstrate the significant potential of CPLM in intelligent packaging, real-time monitoring, and serving as promising sustainable alternatives to conventional petroleum-based materials due to their tunable optical properties and inherent biodegradability (Table 1).

## 5. Challenges and perspectives

### 5.1. Technical hurdles

Despite the promising advancements in applications, the widespread commercialization of photoluminescent cellulose composites faces several technical hurdles that must be addressed.

**5.1.1. Scalability and cost-efficiency.** The transition from laboratory-scale synthesis to industrial production of uniform PL-cellulose composites faces significant economic hurdles. Currently, there is no large-scale industrial production of such materials. The implementation of complex multi-step processing techniques—including surface functionalization and *in situ* synthesis—is anticipated to present substantial scalability challenges and high costs for future industrial-scale manufacturing.<sup>64</sup> Future efforts should focus on developing one-pot synthesis routes, continuous processing methods, and low-cost luminescent composite alternatives.

**5.1.2. Uniform dispersion and compatibility.** Cellulose, as a hydrophilic polysaccharide, exhibits poor compatibility with numerous hydrophobic photoluminescent materials (*e.g.*, quantum dots, rare-earth complexes, and organic fluorophores), leading to pronounced phase segregation and aggregation phenomena.<sup>65</sup> Strategies such as surface silanization, polymer grafting, and the use of amphiphilic compatibilizers have shown promise but require further optimization to achieve uniform dispersion and strong interfacial adhesion.

**5.1.3. Long-term stability.** The operational lifetime of photoluminescent cellulose composites under real-world conditions remains a concern. Key issues include photobleaching of organic fluorophores under UV exposure,<sup>66</sup> hydrolytic degradation of inorganic quantum dots in humid environments,<sup>67</sup> and pH-dependent luminescence quenching of lanthanide complexes.<sup>68</sup> Enhancing the stability will require encapsulation strategies, cross-linking treatments, and the development of



more robust luminescent systems with inherent resistance to environmental stressors.

## 5.2. Future directions

Future research on cellulose-based photoluminescent materials will focus on several core objectives: high performance, intelligent functionality, personalization, and environmental sustainability, necessitating breakthroughs in material, process, and application synergy. Cross-disciplinary collaboration (spanning materials science, bio-technology, and AI) will likely be pivotal for advancing this field.

**5.2.1. Multifunctional composites.** Integrating PL with other functions could construct a multifunctional cellulose composite system.<sup>2,69</sup> Examples of the specific method are as follows: combining antibacterial/antioxidant properties for food active packaging, compounding with elastomers (such as polyurethane) for wearable devices, enhancing barrier performance through nanoclay or graphene reinforcement, developing degradable cellulose-based fluorescent probes for bioimaging, and bonding luminescent signal molecules to indicate the drug release process.

**5.2.2. Sustainable energy-autonomous sensors.** The exploration of CPLM in energy harvesting (e.g., *via* triboelectric nanogenerators using cellulose) could lead to self-powered smart labels.<sup>70</sup> These labels would harness mechanical energy from handling or transport to power their photoluminescence sensing functions, eliminating the need for batteries and further enhancing sustainability.

**5.2.3. Interactive and personalized packaging.** Future CPLM systems may incorporate stimuli-responsive luminescence that changes color or intensity in response to consumer interactions, such as touch (pressure) or breath (moisture).<sup>71</sup> Combined with QR codes or augmented reality (AR) interfaces, this could provide consumers with engaging, personalized product information, authentication assurance, or even entertainment value, enhancing brand experience and trust.

**5.2.4. AI-driven design or application.** Machine learning approaches are being employed to predict optimal composite ratios and processing parameters for cellulose-luminescent systems, enabling data-driven material design.<sup>72</sup> Utilizing synthetic biology approaches, engineered bacteria (e.g., *Komagataeibacter xylinus*) can be reprogrammed to directly secrete luminescent cellulose nanofibers through metabolic pathway modulation. In addition, the integration of CPLM-based sensors with AI algorithms and IoT platforms could enable real-time, *in situ* monitoring of food quality, storage conditions, and supply chain integrity.<sup>73</sup> For instance, CPLM indicators responsive to gases (e.g., NH<sub>3</sub> and CO<sub>2</sub>) or pH changes could wirelessly transmit fluorescence or phosphorescence signals to cloud-based systems. AI-driven data analytics would then predict shelf-life, detect spoilage precursors, and even trigger automated replenishment or recall protocols. This would facilitate truly dynamic “smart packaging” that not only monitors but also communicates and responds.

**5.2.5. Circular systems.** Future research directions will focus more on using agricultural waste (such as rice husk and

sugar-cane bagasse) to extract cellulose and reduce raw material costs, developing water-based or low toxicity solvents (such as ionic liquids and deep eutectic solvents) to replace traditional organic solvents and improving low energy processing technologies (e.g., room temperature molding, 3D printing and electro-spinning) to build circular systems.<sup>74</sup> Based on this, the development of fully biodegradable electronic devices incorporating CPLM represents a promising frontier. Cellulose substrates, combined with eco-friendly conductive inks and luminescent sensors, could form transient electronics for one-time-use packaging. These devices would perform functions like freshness indication, anti-counterfeiting authentication, or dosage tracking in pharmaceuticals, then safely degrade after use, aligning with circular economy principles.

This speculative yet feasible integration highlights the transformative potential of CPLM, suggesting a future where packaging is not merely protective but interactive, communicative, intelligently responsive, and seamlessly sustainable.

## 6. Conclusions

Cellulose-based photoluminescent nanomaterials signify a transformative advancement in sustainable packaging systems, seamlessly integrating renewable material advantages with intelligent sensing capabilities. Despite persistent scalability and stability limitations, recent breakthroughs in nanocellulose engineering and green chemistry offer viable pathways to bridge the gap between laboratory prototypes and practical implementation. To accelerate real-world adoption, strategic research efforts should be focused on developing multifunctional architectures with enhanced processability, while establishing standardized evaluation protocols to ensure commercial feasibility for next-generation intelligent packaging solutions that align with circular economy principles.

## Author contributions

The manuscript was written through the contributions of all authors. All authors have approved the final version of the manuscript.

## Conflicts of interest

There are no conflicts to declare.

## Data availability

No primary research results, software or code have been included and no new data were generated or analysed as part of this review.

## Acknowledgements

We would like to acknowledge funding from the National Natural Science Foundation of China (32471803) and the



Fundamental Research Funds for the Central Universities (2572022CG02).

## Notes and references

1 J. Zhang, Y. Wang, T. Xu, W. Li, Q. Dong, M. Zhang, J. Qi, H. Zhang, X. Wang, W. Liu, L. Zhu and C. Si, *Trends Food Sci. Technol.*, 2025, **160**, 105022.

2 L. Chen, L. Yu, L. Qi, S. J. Eichhorn, A. Isogai, E. Lizundia, J. Y. Zhu and C. Chen, *Nat. Rev. Mater.*, 2025, **10**, 728–749.

3 T. Li, C. Chen, A. H. Brozena, J. Y. Zhu, L. Xu, C. Driemeier, J. Dai, O. J. Rojas, A. Isogai, L. Wågberg and L. Hu, *Nature*, 2021, **590**, 47–56.

4 Q. Wang, R. Zhou, J. Sun, J. Liu and Q. Zhu, *ACS Nano*, 2022, **16**, 13468–13491.

5 X. Wang, J. Guo, H. Ren, J. Jin, H. He, P. Jin, Z. Wu and Y. Zheng, *Trends Food Sci. Technol.*, 2024, **143**, 104289.

6 R. Ramakrishnan, J. T. Kim, S. Roy and A. Jayakumar, *Int. J. Biol. Macromol.*, 2024, **259**, 129194.

7 X. Shi, L. Cui, C. Xu and S. Wu, *Materials*, 2025, **18**, 2919.

8 R. V. Wagh, A. Khan, R. Priyadarshi, P. Ezati and J.-W. Rhim, *Int. J. Biol. Macromol.*, 2023, **233**, 123567.

9 H. Xu, L. Chen, D. Julian McClements, Y. Hu, H. Cheng, C. Qiu, H. Ji, C. Sun, Y. Tian, M. Miao and Z. Jin, *Chem. Eng. J.*, 2022, **432**, 134301.

10 R. J. Moon, A. Martini, J. Nairn, J. Simonsen and J. Youngblood, *Chem. Soc. Rev.*, 2011, **40**, 3941–3994.

11 N. Mittal, T. Benselfelt, F. Ansari, K. Gordeyeva, S. V. Roth, L. Wågberg and L. D. Söderberg, *Angew. Chem., Int. Ed.*, 2019, **58**, 18562–18569.

12 H. Kargarzadeh, M. Mariano, D. Gopakumar, I. Ahmad, S. Thomas, A. Dufresne, J. Huang and N. Lin, *Cellulose*, 2018, **25**, 2151–2189.

13 K. Kobayashi, Y. Ura, S. Kimura and J. Sugiyama, *Adv. Mater.*, 2018, **30**, 1705315.

14 A. Isogai, T. Hänninen, S. Fujisawa and T. Saito, *Prog. Polym. Sci.*, 2018, **86**, 122–148.

15 X. Yang, S. K. Biswas, H. Yano and K. Abe, *ACS Sustainable Chem. Eng.*, 2019, **7**, 9092–9096.

16 N. Mittal, R. Jansson, M. Widhe, T. Benselfelt, K. M. O. Häkansson, F. Lundell, M. Hedhammar and L. D. Söderberg, *ACS Nano*, 2017, **11**, 5148–5159.

17 X. Feng, X. Wang, C. Redshaw and B. Z. Tang, *Chem. Soc. Rev.*, 2023, **52**, 6715–6753.

18 M. Ge, S. Liu, J. Li, M. Li, S. Li, T. D. James and Z. Chen, *Coord. Chem. Rev.*, 2023, **477**, 214951.

19 Y. Gong, Y. Tan, J. Mei, Y. Zhang, W. Yuan, Y. Zhang, J. Sun and B. Z. Tang, *Sci. China: Chem.*, 2013, **56**, 1178–1182.

20 L.-L. Du, B.-L. Jiang, X.-H. Chen, Y.-Z. Wang, L.-M. Zou, Y.-L. Liu, Y.-Y. Gong, C. Wei and W.-Z. Yuan, *Chin. J. Polym. Sci.*, 2019, **37**, 409–415.

21 F. Peng, H. Liu, D. Xiao, L. Guo, F. Yue, H. Würfe, T. Heinze and H. Qi, *J. Mater. Chem. A*, 2022, **10**, 7811–7817.

22 C. Qiu, F. Peng, P. Wu, X. Wang, S. Hu, C. Huang, X. Li, D. Xu, H. Li, P.-C. Ma, P. Chen and H. Qi, *Chem. Eng. J.*, 2024, **485**, 149869.

23 W. Li, S. Wang, Y. Li, C. Ma, Z. Huang, C. Wang, J. Li, Z. Chen and S. Liu, *Carbohydr. Polym.*, 2017, **175**, 7–17.

24 Q. Wu, X. Wang, S. A. Rasaki, T. Thomas, C. Wang, C. Zhang and M. Yang, *J. Mater. Chem. C*, 2018, **6**, 4508–4515.

25 P. Lv, Y. Yao, D. Li, H. Zhou, M. A. Naeem, Q. Feng, J. Huang, Y. Cai and Q. Wei, *Carbohydr. Polym.*, 2017, **172**, 93–101.

26 Z. Song, X. Chen, X. Gong, X. Gao, Q. Dai, T. T. Nguyen and M. Guo, *Opt. Mater.*, 2020, **100**, 109642.

27 W.-Q. Xie, K.-X. Yu and Y.-X. Gong, *Cellulose*, 2019, **26**, 2363–2373.

28 A. A. Altam, J. Xu, M. H. M. A. Shbraen, K. Rehan, H. Yagoub, J. Xu and S. Yang, *Carbohydr. Polym.*, 2017, **168**, 240–246.

29 X. Feng, Y. Tian, G. Gu, C. Wang, S. Shang, X. Huang, J. Jiang, Z. Song and H. Zhang, *Chem. Eng. J.*, 2024, **500**, 156763.

30 W. Zhao, Z. He and B. Z. Tang, *Nat. Rev. Mater.*, 2020, **5**, 869–885.

31 Q. Gao, B. Lü and F. Peng, *Prog. Mater. Sci.*, 2025, **148**, 101372.

32 J. Jiang, S. Lu, M. Liu, C. Li, Y. Zhang, T. B. Yu, L. Yang, Y. Shen and Q. Zhou, *Macromol. Rapid Commun.*, 2021, **42**, 2100321.

33 T. Yang, Y. Li, Z. Zhao and W. Z. Yuan, *Sci. China: Chem.*, 2023, **66**, 367–387.

34 X. Zhang, J. You, J. Zhang, C. Yin, Y. Wang, R. Li and J. Zhang, *CCS Chem.*, 2022, **5**, 2140–2151.

35 X. Zhang, Y. Cheng, J. You, J. Zhang, C. Yin and J. Zhang, *Nat. Commun.*, 2022, **13**, 1117.

36 X. Zhang, Y. Cheng, J. You, J. Zhang, Y. Wang and J. Zhang, *ACS Appl. Mater. Interfaces*, 2022, **14**, 16582–16591.

37 Q. Gao, M. Shi, Z. Lü, Q. Zhao, G. Chen, J. Bian, H. Qi, J. Ren, B. Lü and F. Peng, *Adv. Mater.*, 2023, **35**, 2305126.

38 F. Peng, Y. Chen, H. Liu, P. Chen, F. Peng and H. Qi, *Adv. Mater.*, 2023, **35**, 2304032.

39 K. Jiang, Y. Wang, X. Gao, C. Cai and H. Lin, *Angew. Chem., Int. Ed.*, 2018, **57**, 6216–6220.

40 P. Wang, D. Zheng, S. Liu, M. Luo, J. Li, S. Shen, S. Li, L. Zhu and Z. Chen, *Carbon*, 2021, **171**, 946–952.

41 A. L. Souza, L. M. C. Teixeira, M. B. Freitas-Marques, G. Carneiro and F. M. Pelissari, *Biomass Convers. Biorefin.*, 2024, **15**, 18963–18975.

42 S.-Y. Lee, D. J. Mohan, I.-A. Kang, G.-H. Doh, S. Lee and S. O. Han, *Fibers Polym.*, 2009, **10**, 77–82.

43 S. Maiti, J. Jayaramudu, K. Das, S. M. Reddy, R. Sadiku, S. S. Ray and D. Liu, *Carbohydr. Polym.*, 2013, **98**, 562–567.

44 H. Ji, Z. Xiang, H. Qi, T. Han, A. Pranovich and T. Song, *Green Chem.*, 2019, **21**, 1956–1964.

45 M. Li, P. Yan, J. Liu, Y. Pei, X. Zheng, K. Tang and F. Wang, *Cellulose*, 2022, **29**, 1609–1621.

46 A. N. Frone, S. Berlizoz, J. F. Chailan, D. M. Panaitescu and D. Donescu, *Polym. Compos.*, 2011, **32**, 976–985.



47 E. Robles, I. Urruzola, J. Labidi and L. Serrano, *Ind. Crops Prod.*, 2015, **71**, 44–53.

48 X. Tong, W. Shen, X. Chen, M. Jia and J.-C. Roux, *J. Appl. Polym. Sci.*, 2020, **137**, 48407.

49 H. Tibolla, F. M. Pelissari and F. C. Menegalli, *LWT-Food Sci. Technol.*, 2014, **59**, 1311–1318.

50 M. Li, L.-j. Wang, D. Li, Y.-L. Cheng and B. Adhikari, *Carbohydr. Polym.*, 2014, **102**, 136–143.

51 Q. Lu, L. Lu, Y. Li, Y. Yan, Z. Fang, X. Chen and B. Huang, *ACS Appl. Nano Mater.*, 2019, **2**, 2036–2043.

52 J. F. Luna-Martínez, D. B. Hernández-Uresti, M. E. Reyes-Melo, C. A. Guerrero-Salazar, V. A. González-González and S. Sepúlveda-Guzmán, *Carbohydr. Polym.*, 2011, **84**, 566–570.

53 Z. Yang, S. Chen, W. Hu, N. Yin, W. Zhang, C. Xiang and H. Wang, *Carbohydr. Polym.*, 2012, **88**, 173–178.

54 T. Shi and Y. Lu, *Polymer*, 2020, **189**, 122167.

55 J. Lease, Z. M. Sahin, M. A. A. Farid and Y. Andou, *ACS Sustainable Chem. Eng.*, 2024, **12**, 11789–11796.

56 S. Ravichandran, P. Sengodan, A. Saravanan, S. Vickram and H. Chopra, *Food Chem.*, 2025, **472**, 142888.

57 Z. Yang, X. Yu, B. Huang, J. Li, X. Yan, K. Feng, R. Cai, Y. Yuan, T. Yue and Q. Sheng, *Microchem. J.*, 2025, **212**, 113263.

58 T. Tang, M. Zhang and A. S. Mujumdar, *Food Packag. Shelf Life*, 2024, **46**, 101401.

59 J.-q. Zhan, J.-j. Fu, D.-l. Jin, Y.-w. Yuan, S.-k. Shen, G.-s. Li and Y.-w. Chen, *J. Food Eng.*, 2023, **358**, 111678.

60 Y. Xu, X. Yu, M. Chen, Y. Sun, W. Zhang, Y. Fang, L. Fang, H. Na, F. Liu and J. Zhu, *Chem. Eng. J.*, 2023, **477**, 147272.

61 F. Zhang, Q. Li, C. Wang, D. Wang, M. Song, Z. Li, X. Xue, G. Zhang and G. Qing, *Adv. Funct. Mater.*, 2022, **32**, 2204487.

62 S. Boopasiri, P. Sae-Oui, N. Roamcharern, N. Jangpromma, Y. Ngernyen and C. Siriwong, *Food Packag. Shelf Life*, 2023, **38**, 101102.

63 Y. Zheng, S. He, P. Jin, Y. Gao, Y. Di, L. Gao and J. Wang, *RSC Adv.*, 2022, **12**, 31869–31877.

64 L. Tan, L. Liu, C. Liu and W. Wang, *J. Renewable Mater.*, 2021, **9**, 1897–1911.

65 Y. Kong, T. Lei, Y. He and G. Song, *Food Chem.*, 2022, **390**, 133135.

66 J. Wang, P. Du, Y.-I. Hsu and H. Uyama, *ACS Sustainable Chem. Eng.*, 2023, **11**, 10061–10073.

67 J. Yin, J. Zhang, W. Pan, Z. Wu, F. Wu, J. Dai, J. Luo and C. Chen, *Adv. Funct. Mater.*, 2025, e14590.

68 F. Wang, K. Yao, C. Chen, K. Wang, H. Bai, X.-L. Hao, Q. Wang, X. Dong and W. Liu, *Adv. Funct. Mater.*, 2025, **35**, 2418373.

69 H. Zhong, K. Pan, B. Zhao and J. Deng, *Coord. Chem. Rev.*, 2025, **542**, 216891.

70 X. Meng, C. Cai, B. Luo, T. Liu, Y. Shao, S. Wang and S. Nie, *Nano-Micro Lett.*, 2023, **15**, 124.

71 Z. Zhang, S. Xue, R. Zhou, C. Wang, H. Jayan, J. Li, X. Zou, X. Lu and Z. Guo, *Adv. Funct. Mater.*, 2025, e19324.

72 Y. Xu, Y. Luo, B. Li, W. Jiang, J. Zhang, J. Wei, H. Bai, Z. Wang, J. Ge, R. Lin, Z. Mi, H. Zhang, Y. Tang, M. S. Jones, X. Li, J. Z. H. Zhang and C.-W. Ju, *JACS Au*, 2025, **5**, 3082–3091.

73 N. Mobahi, M. A. Razavi, M. Ekrami, Z. Emam-Djomeh and S. H. Razavi, *Trends Food Sci. Technol.*, 2025, **165**, 105336.

74 C. Huang, H. Yu, Y. Gao, Y. Chen, S. Y. H. Abdalkarim and K. C. Tam, *Adv. Funct. Mater.*, 2025, **35**, 2424591.

